Supplementary Information (SI) for Journal of Materials Chemistry A.
This journal is © The Royal Society of Chemistry 2025

Supporting Information

Steam Activation of Pitch-Based Carbon Fiber for Increasing CO_2 Adsorption Behaviors

Choong-Hee Kim, Seul-Yi Lee*, and Soo-Jin Park*

**Department of Chemistry, Inha University, 100 Inharo, Incheon 22212, South Korea*

* Corresponding author.

E-mail address: sjpark@inha.ac.kr (S. -J. Park), leesy@inha.ac.kr (S. -Y. Lee)

Characterization

The thermodynamic properties of the coffee grounds (precursor) were evaluated by thermal gravimetric and differential thermal analysis (TG-DTA, TG 209 F3, NETZSCH, Germany); the samples were heated up to 1073 K at a rate of 10 K min^{-1} under an N_2 atmosphere. The surface morphologies of all the samples were analyzed by scanning electron microscopy (SEM, Model SU8010, Hitachi Co. Japan). X-ray diffraction (XRD) patterns were measured using the D2 PHASER system (Bruker, Germany) at 30 kV and 10 mA with Cu-Kα radiation. The elemental composition and chemical bond energy on the AC surfaces were analyzed by X-ray photoelectron spectroscopy (XPS, Thermo Scientific, K-Alpha, USA). The CO_2 and N_2 gas adsorption isotherms of the samples were measured with an automatic gas adsorption analyzer (Anton parr, autosorb iQ, USA). The pore size distribution and specific surface area for carbonaceous slit-like pores were determined from the N_2 adsorption–desorption isotherms using the quench solid density functional theory (NLDFT) model and Brunauer–Emmett–Teller (BET) method, respectively.

Adsorption under flue gas condition (gravimetric analysis)

The experimental setup used for the binary mixture gas adsorption measurements is shown in **Fig. S1**. The flue gas adsorption measurements were performed using a thermogravimetric analyzer (TGA, Pyris 1, PerkinElmer, USA). Before the measurements, the samples were heated to 200 K at a rate of 5 K min^{-1} for 6 h in vacuum to remove organic impurities and moisture. In the adsorption stage, the temperature was maintained at 313 K for 1 h under a mixed gas atmosphere containing

15% CO_2 and 85% N_2, which is similar to the flue gas composition of a fossil-fuel power plant. In the desorption stage, a non-heating desorption process was performed for 1 h in vacuum rather than under the flue gas atmosphere.

Adsorption Kinetics study

Adsorption kinetics, cyclic stability, and facile regeneration are equally important factors just like high CO_2 adsorption capacity. To evaluate the adsorption kinetics, here we have measured time-dependent CO_2 adsorption isotherms of SCF-800 using TGA at various temperatures 303, 313, and 323 K under atmospheric pressure (see manuscript). To estimate the CO_2 kinetics, the experimental data was fitted by pseudo-first-order and pseudo-second-order models. Both models explain adsorption rate where pseudo-first-order depends upon the number of adsorption sites (**Eq. S1**) while pseudo-second-order assumes square of the number of adsorption sites (**Eq. S2**).

$$q_t = q_e\left(1 - e^{-k_1 t}\right) \qquad (S1)$$

$$q_t = \frac{1}{\frac{1}{k_2 q_e^2 t} + \frac{1}{q_e}} \qquad (S2)$$

Here, q_e, and q_t denotes adsorption uptakes at equilibrium and time "t", respectively. Additionally, k_1, k_2 denote adsorption rate constants obtained by fitting the experimental data with pseudo-first and pseudo second-order, respectively. Notably, pseudo first-order best fits the experimental data with R^2>0.99 at all temperatures, compared to pseudo second-order, which further indicates the physical adsorption mechanism of CO_2 capture [1, 2]. Additionally, the activation energy was also determined using the following **Eq. S3**.

$$k_1 = A\exp\left(-\frac{E_a}{RT}\right) \qquad (S3)$$

Here "A" is Arrhenius's exponential factor, "E_a" is the activation energy, "R" is the universal gas constant, and "T" represents absolute temperature. A linear fitting graph between the natural log of k_1 and inverse of temperature (*i.e.*, 1/T) was drawn (see manuscript). The activation energy based on obtained fitted parameters was calculated to be 5.41 kJ mol^{-1}, revealing the CO_2 adsorption mechanism predominantly physisorption [3].

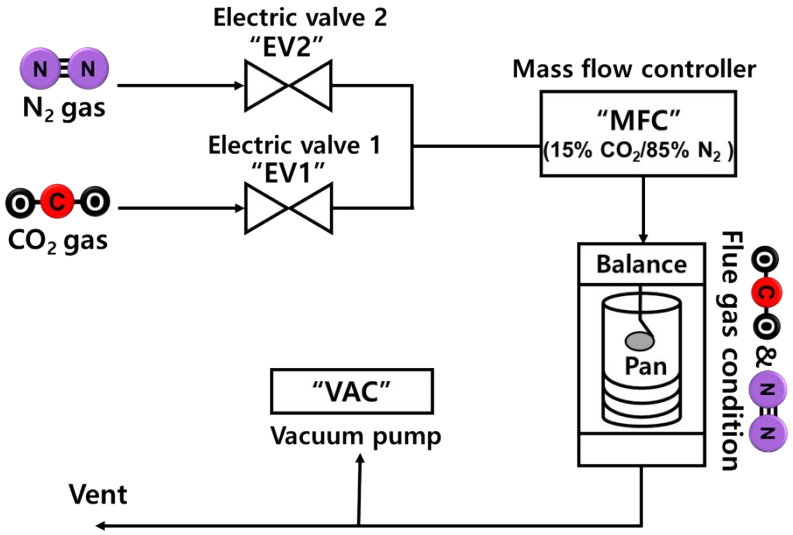

Fig. S1. Experimental setup of the binary mixture gas adsorption (gravimetric analysis) and cycling measurements

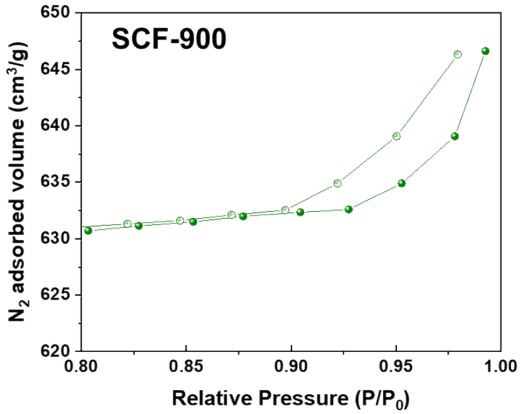

Fig. S2. N_2 adsorption–desorption isotherms of the prepared samples at 77 K in SCF-900 (P/P_0 range of 0.8–0.99

Table. S1 The Elemental compositions determined by XPS and chemical EA

Samples	Elemental analysis (wt.%)			XPS analysis (at.%)	
	C[a]	O[b]	H[c]	C[a]	O[b]
PACF	92.9	3.3	2.0	96.4	3.6
SCF-500	91.5	3.4	1.8	96.2	3.8
SCF-600	92.1	3.9	1.9	95.1	4.9
SCF-700	92.5	4.2	1.8	94.9	5.1
SCF-800	91.8	4.6	1.6	93.6	6.4
SCF-900	91.4	5.2	1.4	92.7	7.2

[a] Carbon contents, [b] Oxygen contents, [c] Hydrogen contents

Table S2. Comparison of the specific surface area of ACFs prepared by physical activation

Samples	Precursor	Activating agents	Activation conditions		Specific surface area (m^2 g^{-1})	References
			Temp. (K)	Time (h)		
SCF-800	Pitch	H_2O	1073	1	1910	This work
SCF-800	Pitch	H_2O	1173	1	2564	This work
HPAC950	Petroleum pitch	CO_2/H_2O	1223	1	2046	[4]
HPAC1000	Petroleum pitch	CO_2/H_2O	1273	1	2506	[4]
ACF-1123	Commercial ACF	H_2O	1123	1	1900	[5]
ACF-1173	Commercial ACF	H_2O	1173	1	3340	[5]
ACF-850-4	Isotropic pitch	CO_2/H_2O	1123	1	1980	[6]
ACF-900-3	Isotropic pitch	CO_2/H_2O	1173	1	2129	[6]
ACF-3	Commercial CF	H_2O	1173	0.6	2650	[7]
ACF-4	Commercial CF	H_2O	1173	0.8	3230	[7]
ETP-200-fiber	Ethylene Tar	CO_2	1173	1	922	[8]
ETP-250-fiber	Ethylene Tar	CO_2	1173	1	1047	[8]

Table S3. Comparison of the CO_2 adsorption capacities of various ACFs

Samples	Precursor	Activating agents	Activation conditions		Specific surface area (m^2 g^{-1})	CO_2 uptakes at 298 K/1 bar (mmol g^{-1})	References
			Temp. (K)	Time (h)			
SCF-800	Pitch	H_2O	1073	1	1910	3.50	This work
SCF-800	Pitch	H_2O	1173	1	2564	2.57	This work
A-PAN/PVDF fiber	PAN/PVDF	H_2O	1173	1	925	2.21	[9]
CF-800-acf	Cellulose	H_2O	1073	1	863	3.78	[10]
CF-850-acf	Cellulose	H_2O	1123	1	1018	3.09	[10]
PCF-500	PAN	Air	773	1	486	2.25	[11]
N-ACF-7/1	Coal-based pitch blend	KOH	973	1	969	2.7	[12]
N-ACF-9/1	Coal-based pitch blend	KOH	973	1	1222	2.6	[12]
aACF	PAN	KOH	1073	1	1565	2.74	[13]
AC-900-3	PAN	KOH	1173	1	1294	3.38	[14]
AC-900-3	PAN/CO	KOH	1173	1	1090	3.28	[14]
MCF-A7/1	Coal	KOH	973	1	1240	3.1	[15]
C800-A1:3	PAN/Cellulose	KOH	1073	1	990	2.99	[16]
PKS-AC	Palm kernel shells	KOH	1123	2	1086	3.39	[17]
NCLK3	Coffee powder	KOH	873	1	840	3.00	[18]
F-600-1	Cow dung	KOH	873	1	1345	3.26	[19]

Table. S4 The kinetic parameters for SCF-800 samples based on CO_2 adsorption data fitting using psuedo first-order and pseudo second-order models at 303, 313, and 323 K.

Samples	Temperature (K)	Psuedo first-order		Psuedo second-order	
		K_1 (min^{-1})	R^2	K_2 (mmol g^{-1} min^{-1})	R^2

SCF-800	303	1.48	0.99816	1.96	0.85541
	313	1.61	0.99224	2.23	0.86988
	323	1.72	0.99801	2.86	0.91047

Reference

1. S.-M. Hong, E. Jang, A. D. Dysart, V. G. Pol and K. B. Lee, *Scientific reports*, 2016, **6**, 1-10.
2. G. Nazir, A. Rehman and S.-J. Park, *Carbon*, 2022, **192**, 14-29.
3. A. E. Creamer, B. Gao and M. Zhang, *Chemical Engineering Journal*, 2014, **249**, 174-179.
4. J. H. Lee, Y. M. Kang and K. C. Roh, *Mater Chem Phys*, 2024, **312**.
5. Y. Yoshikawa, K. Teshima, R. Futamura, H. Tanaka, A. V. Neimark and K. Kaneko, *J Colloid Interf Sci*, 2020, **578**, 422-430.
6. Z. R. Yue, A. Vakili and J. W. Wang, *Chem Eng J*, 2017, **330**, 183-190.
7. H. M. Lee, L. K. Kwac, K. H. An, S. J. Park and B. J. Kim, *Energ Convers Manage*, 2016, **125**, 347-352.
8. H. P. Wang, J. X. Yang, J. Li, K. Shi and X. K. Li, *Sn Appl Sci*, 2019, **1**.
9. Y. J. Heo, Y. F. Zhang, K. Y. Rhee and S. J. Park, *Compos Part B-Eng*, 2019, **156**, 95-99.
10. Y. J. Heo and S. J. Park, *Energy*, 2015, **91**, 142-150.
11. L. Xiong, X. F. Wang, L. Li, L. Jin, Y. G. Zhang, S. L. Song and R. P. Liu, *Energ Fuel*, 2019, **33**, 12558-12567.
12. N. Díez, P. Alvarez, M. Granda, C. Blanco, R. Santamaría and R. Menéndez, *Micropor Mesopor Mat*, 2015, **201**, 10-16.
13. Y. C. Chiang, C. Y. Yeh and C. H. Weng, *Appl Sci-Basel*, 2019, **9**.
14. S. Kocak, C. Akduman, J. Yanik, E. P. A. Kumbasar and A. Cay, *Polymer Engineering & Science*, 2024, **64**, 1355-1364.
15. N. Díez, P. Alvarez, M. Granda, C. Blanco, R. Santamaría and R. Menéndez, *Chem Eng J*, 2015, **281**, 704-712.
16. T. T. Yalçinkaya, A. Çay, Ç. Akduman, E. P. A. Kumbasar and J. Yanik, *J Appl Polym Sci*, 2024, **141**.
17. Gopalan, J., Buthiyappan, A., Rashidi, N. A., Sufian, S., & Abdul Raman, A. A. *Environmental Science and Pollution Research*, 2024, **31**.
18. Plaza, M. G., González, A. S., Pevida, C., Pis, J. J., & Rubiera, F. *Applied energy*, 2012, **99.**
19. Wu, R., & Bao, A. *Journal of CO2 Utilization*, 2023 **68**